Results in Physics 12 (2019) 471–474

Contents lists available at ScienceDirect

Results in Physics

journal homepage: www.elsevier.com/locate/rinp

Analytical analysis of soliton propagation in microcavity wires

U. Al Khawaja[a,*], H. Eleuch[b,c], H. Bahlouli[d,e]

[a] Physics Department, United Arab Emirates University, P.O. Box 15551, Al-Ain, United Arab Emirates
[b] Department of Applied Sciences and Mathematics, College of Arts and Sciences, Abu Dhabi University, Abu Dhabi, United Arab Emirates
[c] Institute for Quantum Science and Engineering, Texas A&M University, College Station, TX 77843, USA
[d] Physics Department, King Fahd University of Petroleum and Minerals, Dhahran 31261, Saudi Arabia
[e] Saudi Center for Theoretical Physics, Dhahran 31261, Saudi Arabia

ARTICLE INFO

Keywords:
Solitons
Quantum wire

ABSTRACT

We propose to explore analytically one of the most promising effects (soliton) for future applications in optical communication processing and memory devices, due to the nonlinearity inside low dimensional semiconductor systems. We focus on soliton propagation in microcavity wires. We derive analytical exact solutions that describe the stationary states of the soliton's profile in the cavity. We present a scheme that gives such profiles for a given external confining potential. The obtained profiles compare favorably with existing experimental and numerical results.

Introduction

Semiconductor microcavities, metamaterials and microcavity wires are recently extensively studied [1–13]. They represent a promising prototype for all optical components in information processing. A panorama of physical effects inside such system has been discovered. Bose-Einstein condensation of polaritons [1,2], polariton superfluidity [3,4], vortices formation [14,15], optical bistability [16,17], polariton multistability [18], wave mixing [19,20], polariton lasers [21], squeezing [22–25], chaos [26,27] and Solitons [28–32]. Solitons are very appealing type of localized excitations for their unique features. In particular, their shape including profile, peak height, and width remain constants throughout the evolution of the soliton's dynamics. This leads to a particle-like behaviour with well-defined conserved momentum, intensity, and energy [33]. Solitons have been explored in several systems such as fluid mechanics [34], atomic physics [35], propagation of laser beams in nonlocal nonlinear media [36], neuronal signals [37]. Solitons can be created in semiconductor microcavity by a pulsed pump beam [38]. Solitons are the results of nonlinear effect inside the semiconductor microcavity. The nonlinearity is generated inside the microcavity by the polariton-polariton interaction. Several numerical studies have explored the proprieties of such solitons [28–31,39]. In general the study is based on solving coupled Nonlinear Schrödinger equations describing the spatiotemporal evolution in 2 + 1 dimensions for the amplitudes of the electromagnetic field and the excitonic mode (see for example Eqs. (1) and (2) in Ref. [28] or Ref. [29]). Our goal here is to derive analytical expressions for soliton profiles. As already mentioned the previous studies were only numerical, finding analytical or approximate solutions will open the door not only for profound understanding of the physics but also to control and to optimize the soliton propagation. Here we propose to study analytically the soliton formation in microcavity wires. In this system the polaritons are confined vertically in a semiconductor cavity. It will be shown here that the system under consideration supports a variety of such solitonic solutions. In addition to accounting for the particular solitonic profiles reported by previous works [4–6], our theoretical model predicts the existence of other solitonic profiles. In the next section we present the theoretical model and the evolution equations for the considered system.

Description of the system and the governing equations

In a simplified scheme, the system described in Fig. 1a of the paper [6] is made of a planar cavity formed by brag mirrors, inside a quantum wire. The system is pumped by a laser in CW mode. In this quantum system interacting excitons and photons can be described by the following two coupled differential equations

$$\frac{\partial E}{\partial t} - i\left(\frac{\partial^2}{\partial x^2} + \frac{\partial^2}{\partial y^2}\right)E + [\gamma_c - i\delta_c - i\Delta - iU(y)]E = i\Omega_R(y)\Psi + E_p e^{ikx} \tag{1}$$

* Corresponding author.
E-mail address: u.alkhawaja@uaeu.ac.ae (U. Al Khawaja).

https://doi.org/10.1016/j.rinp.2018.11.019
Received 10 October 2018; Received in revised form 31 October 2018; Accepted 8 November 2018
Available online 16 November 2018

$$\frac{\partial\Psi}{\partial t}+(\gamma_e-i\delta_e-i\Delta)\Psi+i|\Psi|^2\Psi=i\Omega_R(y)E, \tag{2}$$

where E and Ψ are the averages of the photon and exciton annihilation operators. $E=\langle a\rangle$ and $\Psi=\langle b\rangle$ where a and b are the photonic and the excitonic annihilation operators. They are normalized such that $(\omega_R/g)|E|^2$ and $(\omega_R/g)|\Psi|^2$ are the photon and exciton numbers per unit area. ω_R represents the Rabi frequency and g designs the exciton-exciton interaction. Time t is measured in units of $1/\omega_R$. γ_c and γ_e are the dissipation rates of the cavity and the exciton respectively, normalized to $1/\omega_R$. The coordinates x and y are in unit of $x_0=\sqrt{c/2kn\omega_R}$, where n represents the index of refraction, c is the speed of light in the vacuum and k is the wave number defined by $k=n\omega_0/c$. ω_0 is the external pump frequency. E_p is the normalized amplitude of the external pump defined by $|E_p|=\sqrt{g\gamma_c I_0/(\hbar\omega_0(\omega_R)^2)}$ [40]. I_0 is the intensity of the incident light. $\delta_c=(\omega_c-\omega_0)/\omega_R$ and $\delta_e=(\omega_e-\omega_0)/\omega_R$ are the normalized frequency detunings between the pump frequency ω_0 and the cavity frequency ω_c (respectively the excitonic frequency ω_e).

Note that Δ is not a nabla operator but a parameter which is the detuning between the exitonic and cavity frequencies normalized by the Rabi frequency ω_R.

The effective potential U(y) and the normalized coupling have the following expressions [41]

$$U(y)=U_{bg}\left(1-e^{-(\frac{2y}{W})^8}\right) \tag{3}$$

$$\Omega_R(y)=e^{-(\frac{2y}{W})^8} \tag{4}$$

where W represents the dimensionless wire width.

This model has been solved numerically for the parameters given in Fig. 4 of [6] for the photonic soliton.

Methodology and analytical results

In this section, we present our method of obtaining analytic solutions to the system of Eqs. (1) and (2) with the objective of finding localised solitonic-like solutions as those observed in the experiment. The method is summarised by an inverse procedure where we first find the functional forms of the potentials $U(y)$ and $\Omega_R(y)$ that render the system (1) and (2) to a set of nonlinear Schrd¨inger equations (NLSEs) with cubic nonlinearity. Then we exploit our knowledge of the exact solitonic solutions of the NLSE. Using these solutions, the potentials $U(y)$ and $\Omega_R(y)$ are then determined. The procedure is performed in two steps, at first we determine the y-dependence of the solutions and the potentials. Then we use the potentials back in the original system, Eqs. (1) and (2), to find the x-profiles.

We start by specifying to solutions where x appears only in the phase

$$E(x,y,t)=f(y,t)e^{ikx}, \tag{5}$$

$$\psi(x,y,t)=g(y,t)e^{ikx}. \tag{6}$$

The x-dependence was assumed in this traveling-wave manner to be able to find the y-profiles. Once these are determined, Eqs. (1) and (2) will be resolved with a more general form of the stationary solution where the x-dependence appears also in the f and g functions. With this form of the stationary solutions, Eqs. (1) and (2) take the form

$$-\frac{\partial}{\partial t}f(y,t)-i\frac{\partial^2}{\partial y^2}f(y,t)+if(y,t)(i\gamma\text{ c}+\Delta+\delta\text{ c}+k^2+U(y))+i\Omega_R(y)g(y,t)+E_p=0, \tag{7}$$

$$-i\Omega_R(y)f(y,t)+g(y,t)[ig(y,t)|^2+\gamma\text{ e}-i(\Delta+\delta\text{e})]+\frac{\partial}{\partial t}g(y,t)=0. \tag{8}$$

The crucial step is now to transform the last two equations into two NLSEs. This is performed with the observation that Eq. (7) is a NLSE for $f(y,t)$ but with missing nonlinear term, $|f(y,t)|^2f(y,t)$, and Eq. (8) is a NLSE for $g(y,t)$ but with missing dispersion term, $\frac{\partial^2}{\partial y^2}g(y,t)$. These two missing terms can be compensated for by the external potentials $U(y)$ and $\Omega_R(y)$ if we require that

$$if(y,t)(i\gamma\text{ c}+\Delta+\delta\text{ c}+k^2+U(y))+i\Omega_R(y)g(y,t)+E_p=c_1|f(y,t)|^2f(y,t), \tag{9}$$

and

$$-i\Omega_R(y)f(y,t)+g(y,t)[\gamma\text{ e}-i(\Delta+\delta\text{e})]=c_2^2\frac{\partial^2}{\partial y^2}g(y,t), \tag{10}$$

where c_1 and c_2 are arbitrary constants. Solving Eq. (9) for $\Omega_R(y)$ and Eq. (10) for $U(y)$, we obtain

$$U(y)=\frac{c_1|f(y,t)|^2\text{f}(y,t)-f(y,t)(i\gamma\text{ c}+\Delta+\delta\text{ c}+k^2)-\Omega_R(y)g(y,t)+i\text{Ep}}{f(y,t)}. \tag{11}$$

$$\Omega_R(y)=\frac{-c_2^2\frac{\partial^2}{\partial y^2}g(y,t)+(-2(\Delta+\delta\text{e})-2i\gamma\text{e})g(y,t)}{2f(y,t)}. \tag{12}$$

With these potential profiles, the system (1) and (2) reduce to the following standard NLSEs

$$c_1|f(y,t)|^2f(y,t)+if_t(y,t)-\frac{\partial^2}{\partial y^2}f(y,t)=0, \tag{13}$$

$$ic_2^2\frac{\partial^2}{\partial y^2}g(y,t)+2g_t(y,t)+2i|g(y,t)|^2g(y,t)=0. \tag{14}$$

The last two equations are known to be integrable with many known exact solutions.

As a first example, we consider the fundamental bright soliton solutions of Eqs. (7) and (8)

$$f(y,t)=\text{sech}(y)e^{-it}, \tag{15}$$

$$g(y,t)=\sqrt{2}\,\text{sech}(y)e^{-it}. \tag{16}$$

The external potential profiles then take the form

$$U(y)=-\sqrt{2}(\Delta+\delta_e-\text{sech}^2(y)+\tanh^2(y)), \tag{17}$$

and

$$\Omega_R(y)=-k^2+\Delta-\delta_c+2\delta_e-4\text{sech}^2(y)+2\tanh^2(y), \tag{18}$$

with the values $c_1=-2$ and $c_2=\sqrt{2}$, and $\gamma_e=\gamma_c=E_p=0$. The potentials in this case are shown in Fig.1 for some specific values of the parameters. They are clearly localized as expected for confining potentials.

As another example, we consider the solutions to Eqs. (7) and (8)

$$f(y,t)=-\text{sech}(y)e^{-it}, \tag{19}$$

$$g(y,t)=\tanh(y)e^{-it}, \tag{20}$$

with $c_1=-2$ and $c_2=-i$. For these solutions, the potentials become

$$\Omega_R(y)=-k^2-\Delta-\delta_c-2\text{sech}(y)^2+(\Delta+\delta_e)\sinh(y)^2+\tanh(y)^2, \tag{21}$$

$$U(y)=(\Delta+\delta_e)\sinh(y)+\text{sech}(y)\tanh(y). \tag{22}$$

We turn now to find the x-profile of the fields E and Ψ. To that end, we start with the following form for the fields

$$E(x)=f(x)e^{i\nu t}, \tag{23}$$

and

$$\Psi(x)=g(x)e^{i\nu t}. \tag{24}$$

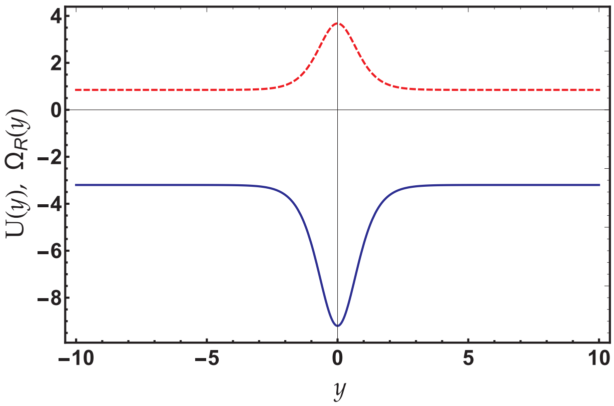

Fig. 1. Potential profiles $U(y)$ with solid blue curve and $\Omega_R(y)$ with dashed red curve given by Eqs. (28). and (29) with parameters: $k = -1,\ \Delta = -2\delta_c = 3,\ \ \delta_e = 0.4$. (For interpretation of the references to colour in this figure legend, the reader is referred to the web version of this article.)

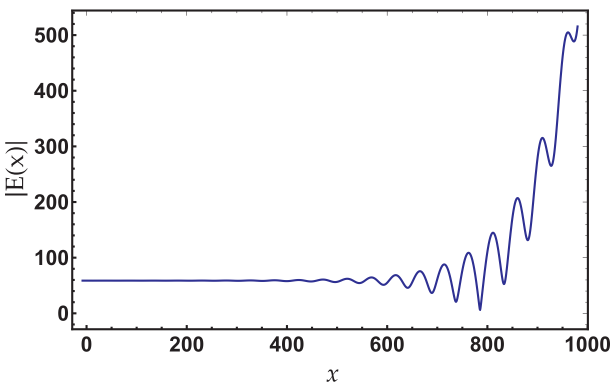

Fig. 2. Solution of Eq. (28), given by Eq. (29) with the parameters: $k = 0.13,\ \ c_1 = 0.01,\ \ c_2 = 0,\ \ E_p = 1,\ \ t = 0$, and $U(0) = 0.000125$.

where v is a real constant. Substituting back in Eqs. (1) and (2), we get

$$f(x)U(y) + g(x)\Omega_R(y) - \frac{\partial^2}{\partial x^2}f(x) = i\,e^{i(kx - vt)}, \tag{25}$$

$$f(x)\Omega_R(y) - g(x)^3 = 0. \tag{26}$$

Substituting for $g(x)$ from the second equation into the first, it reduces to

$$f(x)U(y) + f(x)^{1/3}\Omega_R(y)^{4/3} - \frac{\partial^2}{\partial x^2}f(x) = i\,e^{i(kx - vt)}. \tag{27}$$

The potentials $U(y)$ and $\Omega_R(y)$ may be calculated at $y = 0$ to give rise to the x-profile along that specific line. Furthermore, and to facilitate obtaining analytic solutions, we take the parameters values such that the coefficient of the nonlinear term $f(x)^{1/3}\Omega_R(y)^{4/3}$ is small such that it can be neglected. With this assumption, the last equation simplifies to

$$f(x)U(0) + f(x)^{1/3} - \frac{\partial^2}{\partial x^2}f(x) = i\,e^{i(kx - vt)}. \tag{28}$$

This equation is integrable and admits the following analytic solution

$$f(x) = \left(c_1 e^{2\sqrt{U(0)}\,x} + c_2 + i\frac{E_p}{U(0) + k^2}e^{-ivt + (\sqrt{U(0)} + ik)x}\right)e^{-\sqrt{U(0)}\,x}, \tag{29}$$

where c_1 and c_2 are arbitrary constants. For some specific choices of the parameters, this solution is plotted in Fig. 2. The main feature of this figure shows that the oscillatory amplitude is superimposed on an exponentially increasing function. This feature agrees with the experimental and numerical findings of Refs. [4–6].

Conclusion

We have explored analytically the soliton formation inside a microcavity wire. We have considered a theoretical model of a nonlinear Schrödinger equation with an external effective potential arising from the photons field, as described by Eqs. (1) and (2). We have developed a scheme where for a given confining potential, the exact analytical soliton profile can be obtained. Two specific cases were considered with results shown in Fig. 1. The soliton profiles in the x- and y-directions agree qualitatively with the previously-obtained results, as for instance in Refs. [4–6]. Soliton propagation in microcavity wires opens the door for future advanced applications in optical communication processing and memory devices. It is hoped that our scheme will be useful for further future investigations leading to exact analytic account of the associated nonlinear dynamics of the solitons. This will be pivotal for any technological development that exploits the nonlinear aspect of solitons.

Acknowledgments

We acknowledge the support of King Fahd University of Petroleum and Minerals under research group project RG1503-1 and RG1503-2. We also acknowledge the support of the Saudi Center for Theoretical Physics (SCTP). UAK acknowledges the support of the UAEU UPAR(4), UPAR(6), and UPAR(7) grants.

Appendix A. Supplementary material

Supplementary data associated with this article can be found, in the online version, at https://doi.org/10.1016/j.rinp.2018.11.019.

References

[1] Kasprzak J, Richard M, Kundermann S, Baas A, Jeambrun P, Keeling JMJ, et al. Nat Phys 2006;443:409.
[2] Balili R. Science 2007;316:1007.
[3] Carusotto I, Ciuti C. Phys Rev Lett 2004;93:166401.
[4] Amo A, Sanvitto D, Laussy FP, Ballarini D, del Valle E, Martin MD, et al. Nature 2009;457:291.
[5] Yulin AV, et al. Phys Rev A 2015;91:063820.
[6] Slavcheva G, Gorbach AV, Pimenov A, Vladimirov AG, Skryabin DV. Opt Lett 2015;40:1787.
[7] Mohamed A-BA, Eleuch H. JOSA B 2018;35:47.
[8] Sete EA, Eleuch H. Phys Rev A 2015;91:032309.
[9] Sete EA, Eleuch H. J Opt Soc Am B 2015;32:971.
[10] Sete EA, Eleuch H, Ooi CHR. Phys Rev A 2015;92:033843.
[11] Sete EA, Eleuch H. Phys Rev A 2014;89:013841.
[12] Eleuch H. Eur Phys J D 2008;49:391.
[13] Eleuch H. Eur Phys J D 2008;48:139.
[14] Lagoudakis KG, Wouters M, Richard M, Baas A, Carusotto I, André R, et al. Nat Phys 2008;4:706.
[15] Lagoudakis KG, et al. Science 2009;326:974.
[16] Baas A, Karr JP, Eleuch H, Giacobino E. Phys Rev A 2004;69:023809.
[17] Sete EA, Eleuch H. Phys Rev A 2012;85:043824.
[18] Gippius NA, Tikhodeev SG. J Phys: Condens Matter 2004:S3653.
[19] Savvidis PG, Baumberg JJ, Stevenson RM, Skolnick MS, Whittaker DM, Roberts JS. Phys Rev Lett 2000;84:1557.
[20] Giacobino E, Karrr JPH, Messin G, Eleuch H. CR Phys 2002;3:41.
[21] Schneider Christian, Rahimi-Iman Arash, Kim Na Young, Fischer Julian, Savenko Ivan G, Amthor Matthias, et al. Nature 2013;497:348.
[22] Messin G, Karr JPh, Eleuch H, Courty JM, Giacobino E. J Phys: Condens Matter 1999;11:6069.
[23] Eleuch H, Courty JM, Messin G, Fabre C, Giacobino E. J Opt B 1999;1:1.
[24] Eleuch H, Bennaceur R. J Opt B 2004;6:189.
[25] Sete EA, Eleuch H. Phys Rev A 2010;82:043810.
[26] Eleuch H, Prasad A. Phys Lett A 2012;376:1970.
[27] Eleuch H, Prasad A, Rotter I. Phys Rev E 2013;87:022916.
[28] Salasnich Luca, Malomed Boris A, Toigo Flavio. Phys Rev E 2014;90:043202.
[29] Zhang WL. Opt Exp 2015;23:15762.
[30] Egorov OA. Phys Rev Lett 2009;102:153904.
[31] Sich M. Nat Photon 2012;6:50.
[32] Zhao Xiao-Juan, Guo Rui, Hao Hui-Qin. Appl Math Lett 2018;75:114.
[33] Hasegawa A, Kodama Y. Solitons in optical communications. New York: Oxford University Press; 1995
Mollenauer LF, Gordon JP. Solitons in optical fibers. Boston: Academic Press; 2006

Agrawal GP. Nonlinear fiber optics. 3rd ed. San Diego: Academic Press; 2001
Akhmediev NN, Ankiexicz A. Solitons: nonlinear pulses and beams. London: Chapman and Hall; 1997.
[34] Guo Rui, Hao Hui-Qin, Zhang Ling-Ling. Nonlinear Dyn 2013;74:701.
[35] Meyer Nadine, Proud Harry, Perea-Ortiz Marisa, O'Neale Charlotte, Baumert Mathis, Holynski Michael, et al. Phys Rev Lett 2017;119:150403.
[36] Yang Zhen-Jun, Zhang Shu-Min, Li Xing-Liang, Pang Zhao-Guang. Appl Math Lett 2018;82:64.
[37] Heimburg T, Jackson AD. Proc Natl Acad Sci USA 2005;102:9790.
[38] Hayat A. Phys Rev Lett 2000;109:L509.
[39] carusotto I, Ciuti C. Rev Mod Phys 2013;85:299.
[40] Sich M, et al. Nat Photon 2012;6:50.
[41] Slavcheva G, Koleva MV, Pimenov Alexander. J Opt 2017;19:065404.